Urban Surface Temperatures During the 2003 Heat Wave

B. Dousset[1], F. Gourmelon[2], E. Giraudet[2], K. Laaidi[3], A. Zeghnoun[3], E. Mauri[4]

[1] Hawaii Institute of Geophysics and Planetology, University of Hawaii, Honolulu, Hawaii, USA; [2] Géomer, UMR-6554 LETG CNRS, IUEM Plouzané, France, [3] Institut de Vielle Sanitaire, Saint Maurice, France; [4] Istituto Nazionale di Oceanografica e di Geofisica Sperimentale, Trieste, Italy.

Introduction

In August 2003, a persistent anticyclone over Western Europe generated a heat wave of exceptional strength and duration, resulting in ~ 70 000 deaths (1). From 4 to 13 August, the Paris region experienced nine consecutive days with maximum air temperature (Tair) > 35°C.

A set of 61 NOAA-AVHRR images, one SPOT HRV image, and in-situ meteorological data (Table 1) were used to:

- monitor the diurnal cycle of Land Surface Temperature (LST) during the heat wave
- analyze the temperature variability as a function of land use/cover
- implement indicators of heat exposure to infer the risk of heat related mortality
- demonstrate the relevance of satellite monitoring during heat wave (2).

Data set

Table 1. Data set July 20–August 20, 2003

Measurement systems	Data	Spatial res.	Temporal resolution	Products
NOAA-AVHRR 12, 16, 17 HRPT station of Trieste	**84 images** 07/ 20 – 08/ 20 2003 Ch.1: 0.58 – 0.68 µ Ch.2: 0.72 – 1.00 µ Ch.3 A,B: 3.55, 3.93 µ Ch.4: 10.30 -11.30 µ Ch.5: 11.50 -12.50 µ	1.1 km	2 images/ 24 h NOAA 12,16, 17 →6 images/ 24h	Ch.1, 2 : Albedo, daytime cloudiness Ch.3 vs Ch.4: night cloudiness Ch.1 & Ch. 2: NDVI Ch.4: LST Ch.5: LST
SPOT4 HRV	**1 image** 07/13 2003 11:05 UTC B.1: 0,50 – 0,59 µ B.2: 0,61 – 0,68 µ B.3: 0,78 – 0,98 µ B.4: 1,58 – 1,75 µ	20 m	26 days	B.1 & B.3: NDVI Land cover classification
Weather station Montsouris park	**Meteorological data** 07/ 20 – 08/ 20 2003		Hourly Daily	Tair: +10 cm, +50 cm, +1.50 m Tg: −10 cm Dew-point, water vapour relative humidity wind speed & direction insolation, net radiation Tg −20 cm, −50 cm, −1 m
GIS	Land use layers Paris Planning APUR			Admin. bounderies parks, rivers, industries

The main constraints in retrieving urban LST from satellite sensing are:

- partial absorption of black-body radiation by water vapour and other gases in the atmosphere
- urban surface emissivities being < 1, spatially and spectrally variable (3, 4)
- sub-pixel LST variations and hot spots averaged nonlinearly through Planck's law (5)
- urban canyons trapping energy, increasing the pixel-averaged emissivity
- directional and anisotropic effects due to satellite viewing angle and urban structures (6, 7).

Fig 1. Collocated Tair, LST, RH

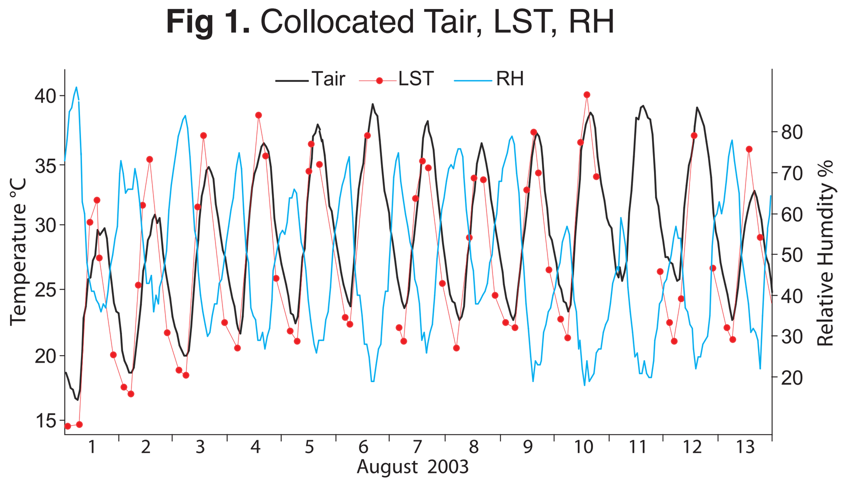

Fig 4. Ch.4 vs Ch.5 Jul 20 - Aug 20

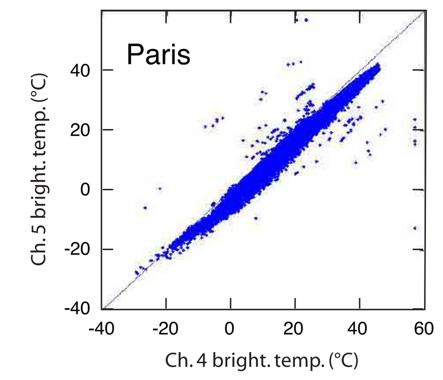

Fig 2. Wind speed

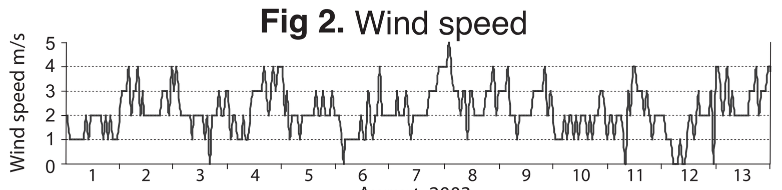

Fig 5. Temporal distribution of images over Paris

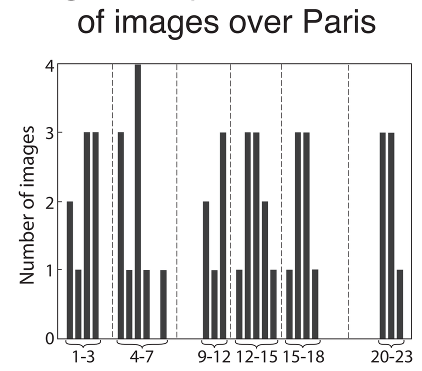

Fig 3. LST vs Tair

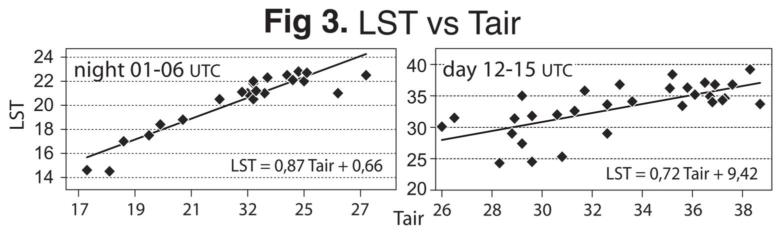

Most images with satellite-zenith angles > 35° were rejected.

Minima of Tair and LST occurred before sunrise at ~ 05:00 UTC. Maximum LSTs occurred at the time of maximum solar irradiance, while maximum Tair lagged by ~3h. The atmosphere was very stable. From 3 to 12 August, the relative humidity (RH) decreased from 38% to 18% during daytime, and 78% to 58% during nighttime (Fig. 1). The wind speed fluctuated between 1 and 4 m/s (Fig. 2.). LST vs. Tair (Fig. 3) displays a linear correlation coefficient of 0.92 by night and 0.68 by day, reflecting stronger sub-pixel variations of surface cover.

From July 20 to August 20, the differential atmospheric attenuation (Fig. 4) yielded a negligible water vapor correction of < 1°C at night and 1°C–1.7°C during the day for temperatures of 30°C and 40°C.

Median LST images were constructed from 50 NOAA-AVHRR images for Paris and 24 for London over six time intervals of satellite passes during the heat wave (Fig. 5).

Surface temperature variability in Paris and London

Fig 6. Average LST images over the diurnal cycle in Paris (a) and London (b) from 4–13 Aug 2003

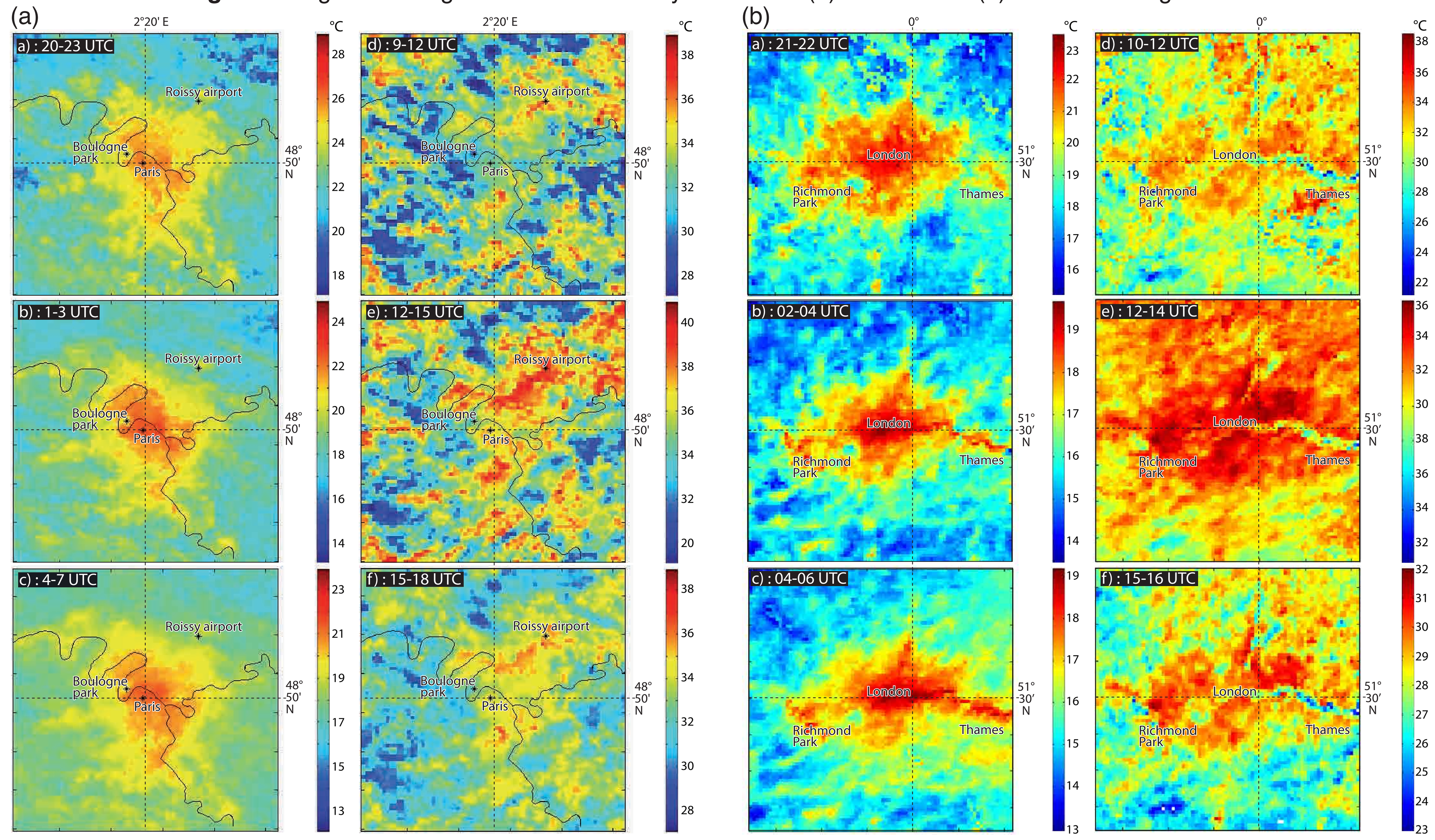

Median LST images (Fig. 6 a, b) reveal contrasted day/night patterns, reflecting different rates of heating and cooling between urban and suburban areas. In Paris, nighttime images show Urban Heat Islands (UHI) up to 8°C. The LST distribution is well correlated with increasing built density (Fig. 7).

Fig 7. Paris land use classification

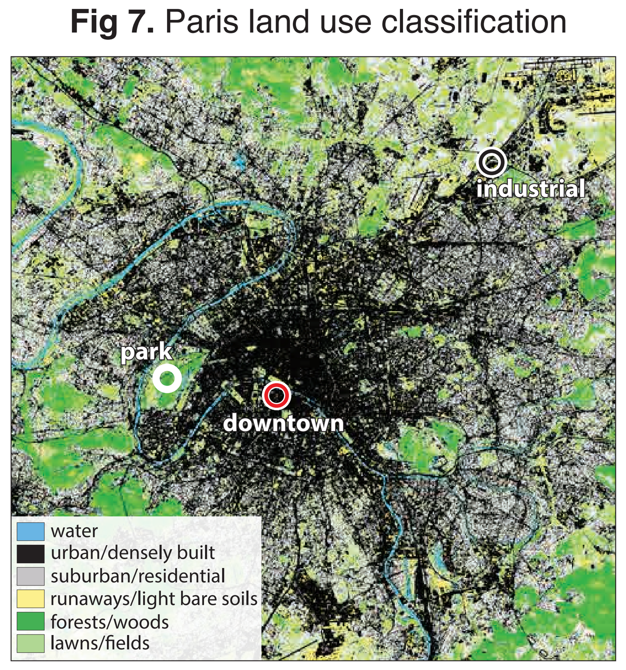

SPOT-4 HRV, 13 July 2003 1105 UTC

Fig 8. LST diurnal cycles at 3 sites

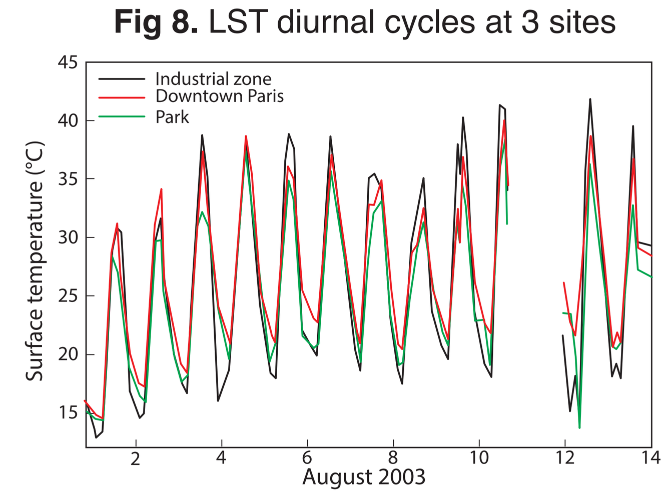

Fig 9. UHI intensity

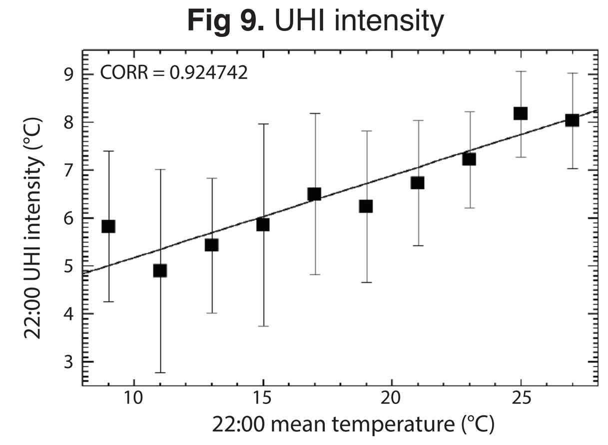

Fig 10. LST normal vs heat wave

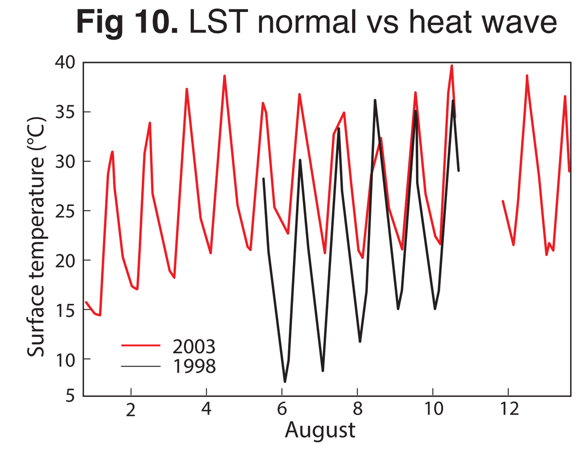

Fig 11. Afternoon LST vs NDVI

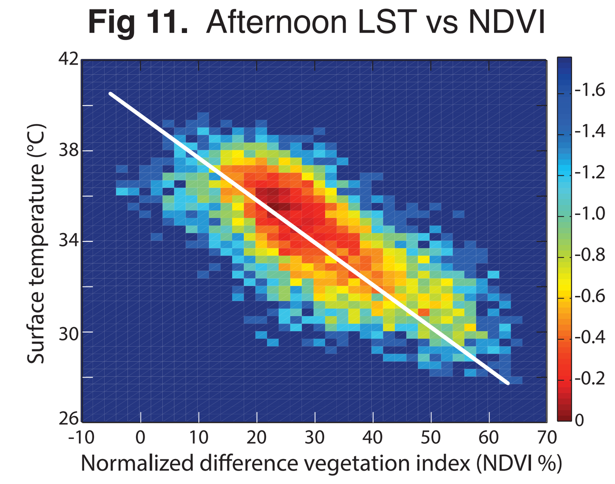

In Paris, daytime thermal anomalies in densely built and industrial suburbs convey variations of the surface heat balance related to surface thermal inertia and soil moisture availability (Fig.8). During the heat wave the UHI intensity increases with large-scale ambient temperature (8) (Fig. 9). Temperature amplitudes of the summer of 1998 vs. 2003 confirm the impact of nighttime minimum temperatures on the heat wave process (Fig. 10). Each % of vegetation photosynthesis decreases the LST by -0.2°C (Fig. 11). Small/large parks are 2-3°C/4-5°C cooler than built surroundings.

Multi-layers of land use maps over median thermal images enable identification of risk factors areas (Fig. 12, Fig. 13).

Fig 12. UHI and land use

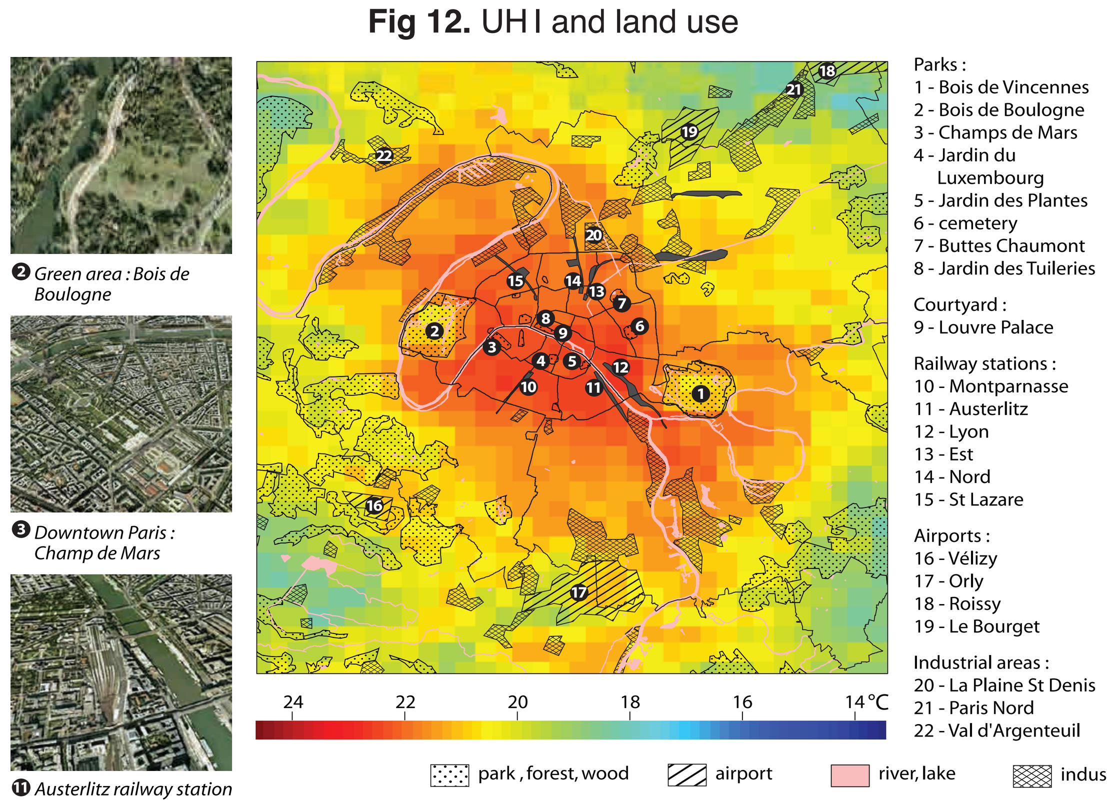

Fig 13. Thermal anomalies and land use

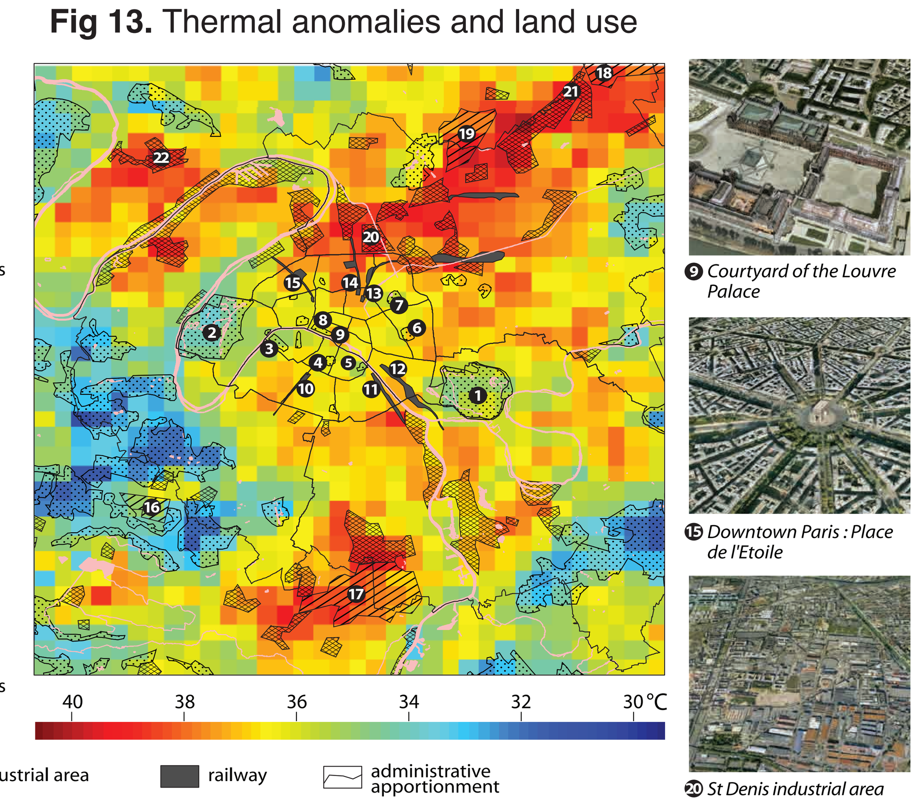

Heat related mortality in Paris

In August 2003, the excess mortality reached +141% in the Paris region, with 4867 heat-related deaths (Fig. 14). The French Institute for Public Health Surveillance conducted a 482 cases-controls study to identify mortality risk factors for elderly people > 65 years, living in Paris during the heat wave. Then, using 61 NOAA-AVHRR images over 13 days, ~29000 thermal indicators were extracted at 482 addresses (Fig. 15), enabling the estimation of the relative impact of heat exposure on elderly people and the time lag between heat exposure and death (9) (Table 2).

Fig 14. Temperature and mortality (IVS)

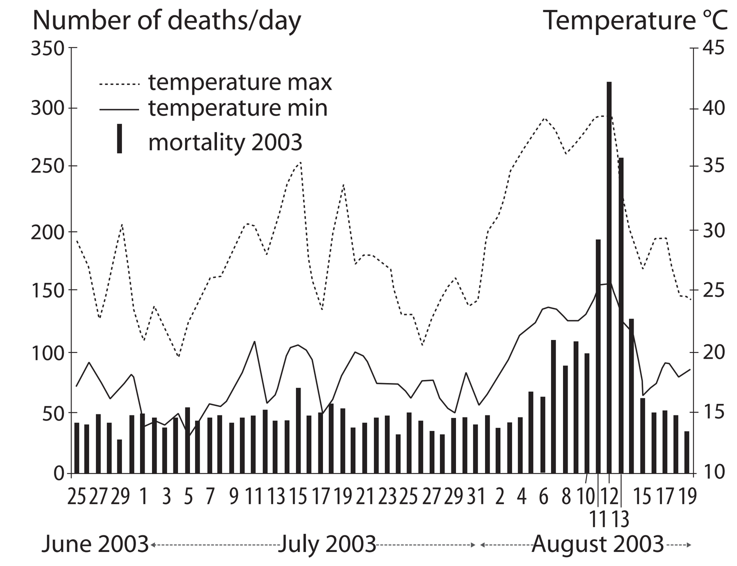

Fig 15.

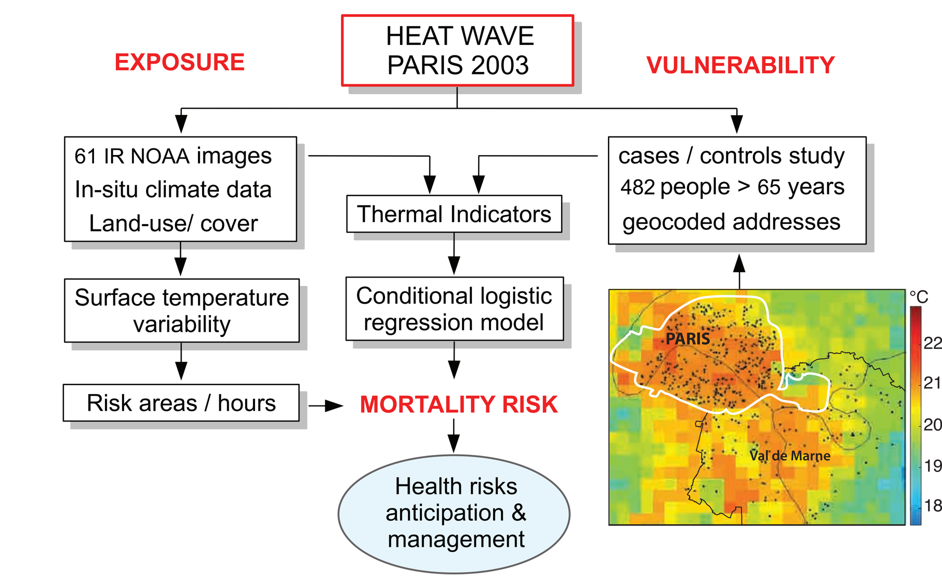

0.5°C night-time increase during a week doubles the risk of death

Table 2. Mortality odds ratios / thermal indicators and time lag

Satellite thermal indicators	Temperature difference between cases and controls	OR (95% CI)
From August 1 to 13		
Average Maximum LST	0.97 °C	1.29 (0.61, 2.72)
Average Minimum LST	**0.41** °C	**2.17** (1.14, 4.16)
Average Mean LST	0.37 °C	1.71 (0.94, 3.11)
From 6 days before death to the day of death		
Average Maximum LST	0.92 °C	0.93 (0.51, 1.69)
Average Minimum LST	**0.51** °C	**2.24** (1.03, 4.87)
Average Mean LST	0.46 °C	1.34 (0.71, 2.51)
From 2 days before death to the day of death		
Average Maximum LST	1.25 °C	0.91 (0.56, 1.47)
Average Minimum LST	0.68 °C	1.40 (0.67, 2.91)
Average Mean LST	0.67 °C	1.06 (0.60, 1.89)
The day before death		
Maximum LST	1.51 °C	1.05 (0.77, 1.42)
Minimum LST	0.85 °C	1.17 (0.70, 1.96)

Key findings

- Contrasted nighttime and daytime heat island patterns, related to surface characteristics and land use
- Cooling impact of urban parks
- Significance of elevated nocturnal minimum temperatures on heat wave intensity and excess mortality
- Relative impact of heat exposure on elderly people and time lag between exposure and death, with a 0.5°C minimum temperature increase during 6 consecutive days doubling the risk of death
- Relevance of urban satellite monitoring during heat waves to identify risk areas, providing rapid response for public health decisions and criteria for urban climate mitigation strategies.

References

1. Robine JM, Cheung S, Le Roy S, Van Oyen H, Griffiths C, Michel JC, Herrmann F. 2008. Death toll exceeded 70,000 in Europe during the summer of 2003. CR Biology 331: 171–178.
2. Dousset B, Gourmelon F, Laaidi K, Zeghnoun A, Giraudet E, Bretin P, Mauri E, Vandentorren S. 2011. Satellite monitoring of summer het waves in the Paris metropolitan area, Int. J. Climatology, 31, 313–323.
3. Dash P, Gottsche FM, Olesen FS, Fischer H. 2002. Land surface temperature and emissivity estimation from passive sensor data: theory and practice– current trends. Int. J. Remote Sens., 23 (13), 2563–2594.
4. Gustafson WT, Gillespie AR, Yamada GJ. 2006. Revisions to the ASTER temperature/emissivity separation algorithm. 2nd Intern. Symposium on Recent Advances in Quantitative Remote Sensing, Univ. of Valencia, Torrent, Spain.
5. Dousset B, Flament P, Bernstein R. 1993. Los Angeles fires seen from space. EOS Trans. AGU, 74, 33, 37–38.
6. Voogt JA, Oke TR. 1998. Effects of urban surface geometry on remotely sensed surface temperature. Int. J. Remote Sens., 19, 895–920.
7. Lagouarde JP, Moreau P, Irvine M, Bonnefond JM, Voogt JA, Solliec F. 2004. Airborne experimental measurements of the angular variations in surface temperature over urban areas: case study of Marseilles. Remote Sens. Environ., 93, 443–462.
8. De Ridder K, Maiheu B, Lauwaet D, Ceriola G, Keramitsoglou I, Montero-Herrero E, Radius A, Dousset B, et al. 2012. Urban heat island intensity of Paris during the Summer 2003 heat wave. In Proc. 8th Int. Conf. Urban Climates, Dublin.
9. Laaidi K, Zeghnoun A, Dousset B, Bretin P, Vandentorren S, Giraudet E, Beaudeau P. 2012.The impact of heat islands on human health in Paris during the August 2003 heat wave, Environ. Health Persp., 120(2), 254–259.